High-fidelity Simulations of Oblique Detonation Waves

Sebastian S. Abisleiman, Ral Bielawski, Venkat Raman
University of Michigan
Ann Arbor, Michigan, United States

1 Background & Introduction

To realize oblique detonation wave (ODW) usage in propulsion devices, ODW structure and stability must be further understood. In particular, the behavior of triple points and fluid instabilities in the flow field are studied here through numerical simulation of an ODW. ODWs are an alternative form of combustion for application in air-breathing hypersonic vehicles utilizing oblique detonation wave engines (ODWEs) [1, 2]. In practical applications, there are many advantages to ODWs as there are no moving components as well as the potential for thrust production at higher efficiencies than comparable deflagration based engines. ODWs can occur when a reactive gas mixture impinges on a wedge surface and a shock-to-detonation transition is made. Depending on wedge angle and post-shock conditions, the inflow reactants will detonate and form an ODW structure that will either have a smooth transition or an abrupt transition from OSW to detonation wave through a multi-wave point connecting the two.

Previous numerical [3–7] and experimental [8–11] studies have looked at the oblique detonation wave structure and initiation. Li et al. [3] conducted the first ODW numerical simulation looking at structure and stability. Further numerical simulations have investigated flow features related to shock wave, deflagration, and transverse wave interactions [5–7]. However, studies often ignore the effects of viscosity, use simple chemical kinetics mechanisms, and simulate with coarse spatial resolution. As the study of ODWs develops it is critical that viscosity, complicated chemistry, and fine spatial resolution is accounted for to better understand the structure and stability of ODWs. With sufficient chemical complexity and spatial refinement, triple point instabilities are observed in numerical simulation on the detonation surface. Therefore, this work represents some of the first two-dimensional numerical studies of oblique detonation waves at extremely high-resolution with complex chemical kinetics and is a critical step to elucidating the dynamic behavior of ODWs.

2 Flow Configuration

A schematic of a wedge-induced oblique detonation wave in a combustible mixture is shown in Fig. 1. With the x-direction aligned along the wedge, computationally the inflow is directed to impact the lower boundary at an angle to simulate flow impinging upon a wedge as shown in Fig. 1. The domain dimensions are x = 4 cm and y = 1 cm. The lower boundary contains a section ahead of the wedge for supersonic outflow with a zero-gradient boundary condition, while the wedge utilizes a no-slip boundary condition for velocity. Supersonic inflow is present in the left and top boundaries while the right boundary is a zero-gradient supersonic outflow. The ODW is formed with OSW combustion coupling when the post-shock conditions has reached a sufficiently high temperature to initiate detonation. The inflow reactants are a hydrogen-air mixture at an equivalence ratio of $\phi = 1$. The inflow parameters are M = 5, T = 500 K, and p = 1 atm with a wedge angle of $\theta = 30°$.

Correspondence to: sabislei@umich.edu

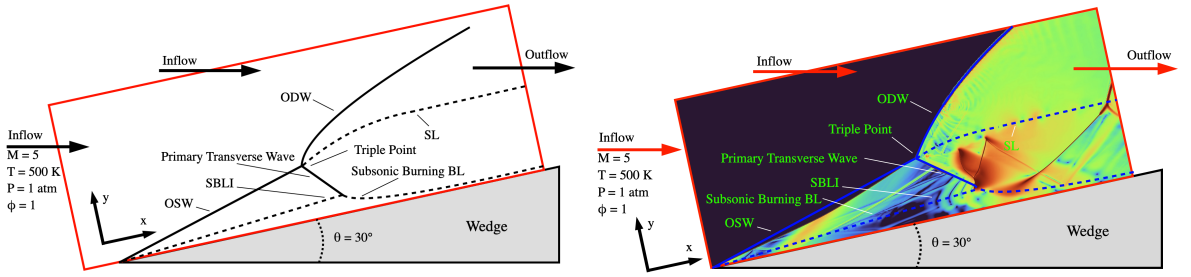

Figure 1: Left: Schematic of wedge-induced oblique detonation waves, Right: Schematic of wedge-induced oblique detonation waves with 3.125 μm resolution simulation results overlaid.

3 Numerical Approach

A high fidelity numerical simulation approach is utilized to study ODW behavior. The governing equations include mass, momentum, and energy conservation equations augmented with species conservation equations, integrating chemical reactions. The ideal gas equation of state is used to close the system of equations. The Navier-Stokes equations for compressible, reacting fluid flows is utilized within UMdetFOAM for numerical simulation [12]. The MUSCL (Monotonic Upwind Scheme for Conservation Laws)-based HLLC (Harten- Lax-van Leer-Contact) and HLLE (Harten-Lax-van Leer-Einfeldt) schemes are utilized in separate simulations for spatial discretization of convective flux. A second-order Runge-Kutta multi-stage method is used for temporal discretization. Diffusion terms are discretized through the Kurganov, Noelle, and Petrova (KNP) method and chemical reactions are computed using Cantera [13] [14].

The solver is parallelized utilizing MPI-based domain decomposition and is executed on approximately 3000 cores in the current study. The detailed chemistry is modeled for hydrogen-oxygen combustion with a nitrogen diluter using a 9-species 19-reaction chemical mechanism derived from Mueller et al. using Cantera-based subroutines [15]. Capturing complex chemistry has been shown to be critical to study formation of instabilities in the oblique detonation wave flow field [16]. Adiabatic and no-slip boundary conditions are applied at the wedge surface. The finest resolutions in the ODW simulations utilizing HLLC and HLLE are 3.125 μm and 781.125 nm respectively. With the utilization of HLLC flux in the 3.125 μm case, there may be issues with carbuncles in HLLC's treatment of shock waves due to the lack of diffusion normal to the shock and therefore generation of spurious oscillations in the simulation that may have impact on acoustic wave formation. Therefore, a more dissipative HLLE flux is utilized in the subsequent 781 nm case with higher resolution to compensate for its more diffusive effects and to more accurately simulate the flow-field. In the 3.125 μm case , there are approximately 200 cells across the detonation induction length to resolve this feature of the detonation. With adaptive mesh refinement (AMR) the case with HLLC flux contains approximately 8 million cells while the case with HLLE flux contains approximately 50 million cells.

4 Results and Discussion

At the simulated conditions, an ODW presents in an abrupt shock-to-detonation transition with a primary and secondary transverse wave present, along with a train of left running transverse waves that later encounter right running transverse waves that form a separate cellular detonation region. Utilizing AMR the finest resolution in this case is 3.125 μm.

In Fig. 2 and Fig. 3 Kelvin-Helmholtz (KH) instabilities can be seen in the flow-field behind the detonation emanating from the triple points at the detonation surface. The KH instabilities are most clearly

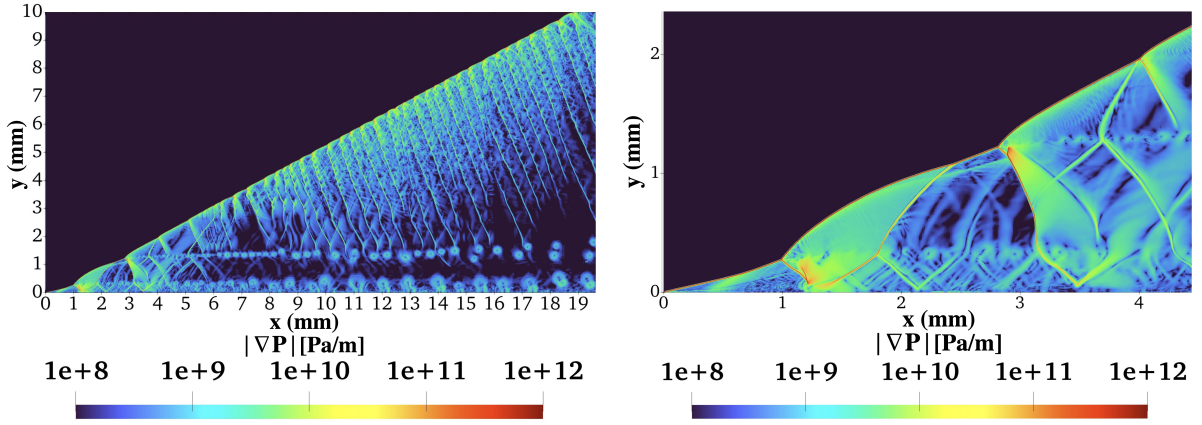

Figure 2: Contour plots of pressure gradient using 3.125 μm resolution, Left: Pressure gradient of entire simulation domain, Right: Magnified view in primary transverse wave region.

visible in the shear layers emanating from the first two triple points. Subsequent KH instabilities intersect transverse waves downstream causing reflection of the transverse waves. The KH vorticies closest to the viscous wall break down due to interaction with the subsonic boundary layer. In the triple-point regions shown in Fig. 3, baroclinic torque is significantly large due to the gradients of pressure from the leading shock and density gradients from combustion behind the transverse waves being misaligned. This leads to unequally accelerated fluid and vortex generation. Baroclinic torque represents the generation of vorticity and thus the KH instabilities shed from the triple point locations. Transverse wave reflection can be seen off the shear layer caused by the KH instabilities in Fig. 2. Upon closer inspection of the leading OSW and primary transverse wave, the OSW can be seen in more detail with pressure oscillations or acoustic waves moving towards the primary transverse wave in Fig. 2.

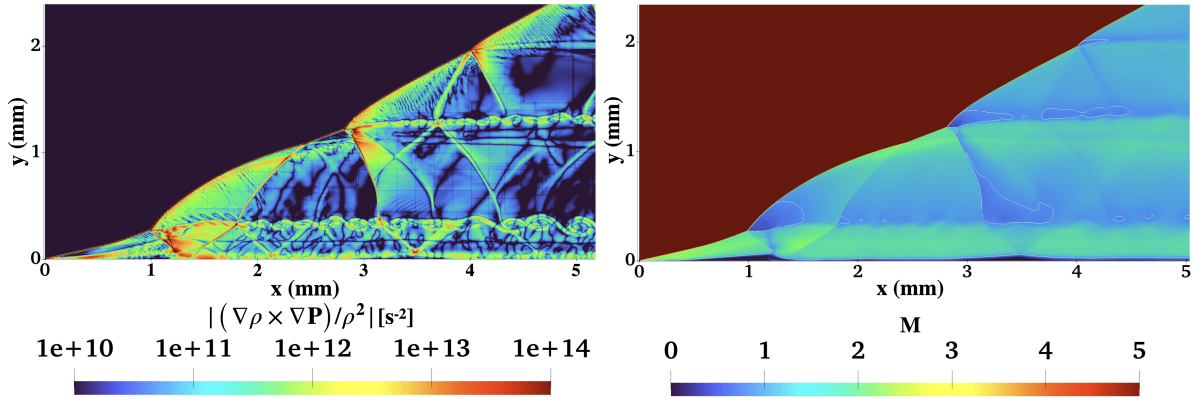

Figure 3: Contour plots in the primary transverse wave region using 3.125 μm resolution, Left: Baroclinic torque, Right: Mach number with regions of sonic flow colored white.

Shock-boundary layer interaction (SBLI) is also present where the boundary layer burning and the primary transverse wave meet at the wall, causing a subsonic re-circulation region at the wall. In Fig. 3, subsonic regions are outlined in white contour and show the subsonic regions of SBLI as well as the subsonic regions behind the triple points and the locally over-driven detonation in those regions. In the cellular detonation region shown in Fig. 4, left running and right running transverse waves can be seen colliding. Upon collision, spikes of higher density fluid, similar to the Rayleigh-Taylor (RT) instability, can be seen in Fig. 4 as the detonation surface bulges to move into the lower density incoming reactants. This behavior is similar to the behavior seen in other 2D detonation channel simulations. The spikes

move downstream and form deformed KH vortices.

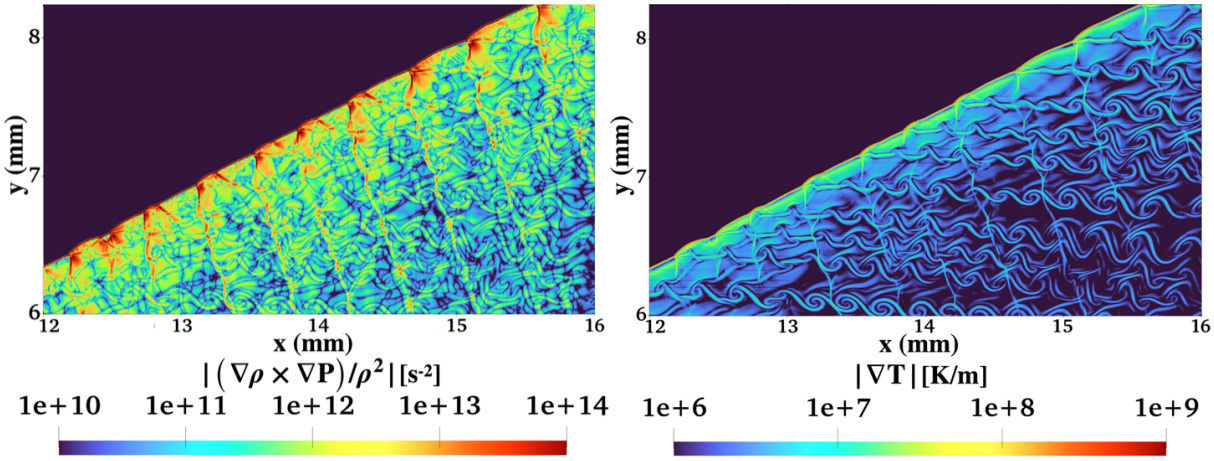

Figure 4: Contour plots in the cellular detonation region using 3.125 μm resolution, Left: Baroclinic torque, Right: Temperature gradient

In Fig. 2, acoustic waves can be seen travelling along the OSW and behind the triple point over-driven detonation region. There is thought that coalescing of these acoustic waves might be the driver of transverse wave formation in ODWs.

At the simulated conditions, an ODW presents in an abrupt shock-to-detonation transition with a primary and secondary transverse wave present, along with KH instabilities forming a shear layer. Utilizing AMR the finest resolution in this case is 781 nm.

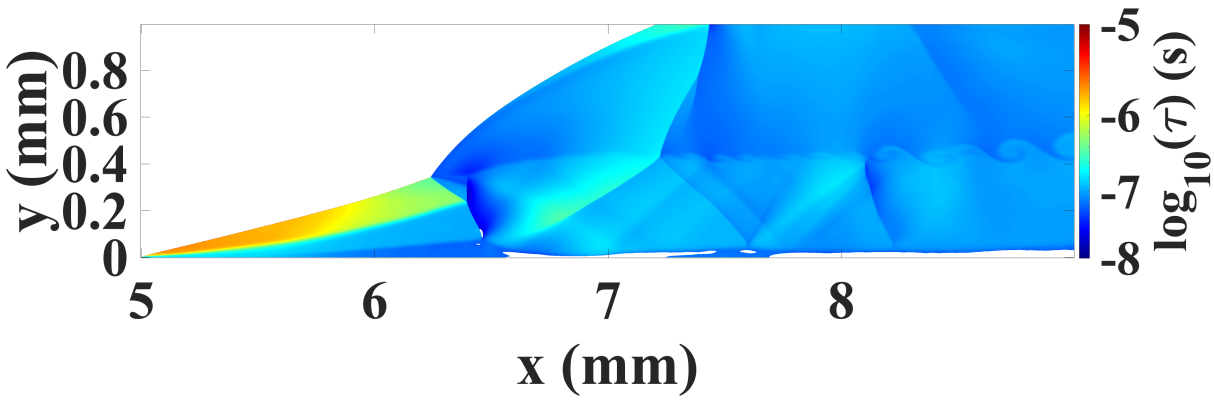

Figure 5: Contour plot of ignition delay in the primary transverse wave region using 781 nm resolution with local composition and temperature in a constant-volume homogeneous reactor.

Ignition delay is computed using the Hon Mueller chemical kinetics mechanism with stoichiometric hydrogen-air mixture utilizing the one-dimensional homogeneous reactor in Cantera and detecting ignition delay time as the time of peak temperature gradient. In Fig. 5, the short ignition delay is found in the regions of strong detonation behind the primary transverse wave, behind the detonation surface, and in the subsonic burning boundary layer. Long ignition delay is found in the regions of the OSW prior to combustion and expansion waves off the subsonic burning boundary layer.

In Fig. 6, the induction length reaches low values of 10 nm near regions of high temperature and pressure in the subsonic boundary layer burning and is higher in the detonation region with values around 100 μm. In order to properly resolve the detonation in these regions, it is expected that at least there are 10

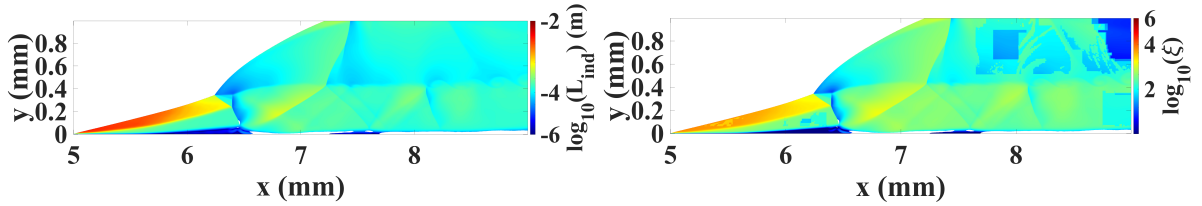

Figure 6: Contour plot of the primary transverse wave region using 781 nm resolution, Left: Induction length, Right: Induction length resolution ratio.

control volumes within the induction region or that the induction length in one cell must be 10 times larger than the size of the cell. This ratio of induction length resolution ξ can be seen in Fig. 6, where in the worst case there are approximately 20 cells per induction length in the strong detonation regions near the primary transverse wave and detonation surface. In the downstream regions there are generally in excess of 100 cells per induction length.

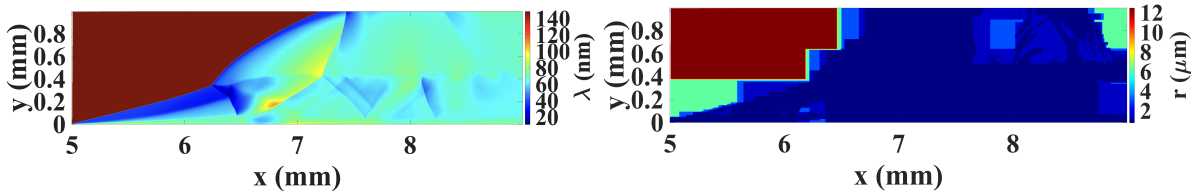

Figure 7: Contour plot of primary transverse wave region using 781 nm resolution, Left: Mean free path, Right: Mean inter-molecular distance.

Upon comparison in Fig. 7, it is evident that the mean inter-molecular distance is larger than the mean free path in the simulation. The mean inter-molecular distance is dependent on cell size and this is shown as the regions on low particle spacing are closely correlated with regions of high AMR. The mean free path decreases in regions of high temperature and pressure after shock waves and in regions of detonation of high heat release rate. The mean free path is the shortest in the OSW prior to combustion due to high pressures and temperatures without combustion and then again immediately after detonation behind the primary transverse wave and detonation surface where combustion is occurring and temperatures and pressures are at their peak.

5 Conclusion

Oblique detonation waves were studied with, complex chemical kinetics, at 3.125 μm and 781 nm resolution using HLLC and HLLE fluxes respectively. Triple-point instabilities from the transverse waves can be seen in the largely stationary primary transverse wave region and in the moving cellular detonation region. KH instabilities seem to emanate from the triple-point instabilities where there are peak regions of baroclinic torque. Ignition delay decreases in the regions of strong detonation and the induction length increases in the OSW and expansion regions. Mean free path increases greatly in regions of expansion and decreases sharply in regions of the OSW and strong detonation where temperatures and pressures are high. The HLLE 781 nm study was able to show more clearly some of the key chemical parameters like ignition delay, induction length, and mean free path in the primary transverse wave region, while the HLLC 3.125 μm study more aptly shows the larger flow field features such as the KH instabilities, triple-points, and cellular detonation region. In future studies, the aforementioned features could be simulated at higher resolutions to study triple-point and other instability formation.

References

[1] P. Wolański, "Detonative propulsion," *Proc Combust Inst.*, vol. 34, no. 1, pp. 125–158, 2013.

[2] K. Kailasanath, "Review of propulsion applications of detonation waves," *AIAA J.*, vol. 38, no. 9, pp. 1698–1708, 2000.

[3] C. Li, K. Kailasanath, and E. S. Oran, "Detonation structures behind oblique shocks," *Phys. Fluids*, vol. 6, no. 4, pp. 1600–1611, 1994.

[4] J. Verreault, A. J. Higgins, and R. A. Stowe, "Formation of transverse waves in oblique detonations," *Proc Combust Inst.*, vol. 34, no. 2, pp. 1913–1920, 2013.

[5] Y. Liu, Y.-S. Liu, D. Wu, and J.-P. Wang, "Structure of an oblique detonation wave induced by a wedge," *Shock Waves*, vol. 26, pp. 161–168, Mar. 2016.

[6] S. Miao, D. Xu, T. Song, and J. Yu, "Shock wave-boundary layer interactions in wedge-induced oblique detonations," *Combust Sci Technol*, vol. 192, no. 12, pp. 2345–2370, 2020.

[7] K. Iwata, O. Imamura, K. Akihama, H. Yamasaki, S. Nakaya, and M. Tsue, "Numerical study of self-sustained oblique detonation in a non-uniform mixture," *Proc Combust Inst.*, vol. 38, no. 3, pp. 3651–3659, 2021.

[8] C. Viguier, L. F. F. da Silva, D. Desbordes, and B. Deshaies, "Onset of oblique detonation waves: Comparison between experimental and numerical results for hydrogen-air mixtures," *Symp. (Int.) Combust.*, vol. 26, no. 2, pp. 3023–3031, 1996.

[9] J. Kasahara, T. Arai, S. Chiba, K. Takazawa, Y. Tanahashi, and A. Matsuo, "Criticality for stabilized oblique detonation waves around spherical bodies in acetylene/oxygen/krypton mixtures," *Proc Combust Inst.*, vol. 29, no. 2, pp. 2817–2824, 2002.

[10] J.-C. Broda, "An experimental study of oblique detonation waves," *ProQuest Dissertations and Theses*, p. 151, 1993.

[11] D. A. Rosato, M. Thornton, J. Sosa, C. Bachman, G. B. Goodwin, and K. A. Ahmed, "Stabilized detonation for hypersonic propulsion," *Proc Natl Acad Sci U S A*, vol. 118, no. 20, p. e2102244118, 2021.

[12] T. Sato, S. Voelkel, and V. Raman, "Detailed chemical kinetics based simulation of detonation-containing flows," vol. Volume 4A: Combustion, Fuels, and Emissions, 2018.

[13] C. J. Greenshields, H. G. Weller, L. Gasparini, and J. M. Reese, "Implementation of semi-discrete, non-staggered central schemes in a colocated, polyhedral, finite volume framework, for high-speed viscous flows," *Int J Numer Methods*, vol. 63, no. 1, pp. 1–21, 2010.

[14] D. G. Goodwin, H. K. Moffat, I. Schoegl, R. L. Speth, and B. W. Weber, "Cantera: An object-oriented software toolkit for chemical kinetics, thermodynamics, and transport processes." `https://www.cantera.org`, 2022. Version 2.6.0.

[15] M. A. Mueller, T. J. Kim, R. A. Yetter, and F. L. Dryer, "Flow reactor studies and kinetic modeling of the H_2/O_2 reaction," *Int. J. Chem*, vol. 31, no. 2, pp. 113–125, 1999.

[16] H. Guo, X. Jia, N. Zhao, S. Li, H. Zheng, C. Sun, and X. Chen, "The formation and development of oblique detonation wave with different chemical reaction models," *Aerosp. Sci. J.*, vol. 117, p. 106964, 2021.